EPJ Web of Conferences **309**, 03016 (2024) https://doi.org/10.1051/epjconf/202430903016
EOSAM 2024

Mesh-Based Double-Sided Freeform Lens Optimization

Yuou Sun[1,⋆], *Bailin* Deng[2,⋆⋆], and *Juyong* Zhang[1,⋆⋆⋆]

[1] *School of Mathematical Sciences, University of Science and Technology of China, China*
[2] *School of Computer Science and Informatics, Cardiff University, UK*

Abstract. We present a mesh-based method for optimizing double-sided freeform lenses to control their caustic effects. Unlike traditional single-sided approaches, we optimize both sides of the lens simultaneously, using a bijective correspondence between the two sides to control light refraction paths. Our approach balances image fidelity, geometric compatibility, and physical constraints. Results demonstrate the method's capability to accurately produce intricate light patterns, opening new possibilities in optical applications.

1 Introduction

In the field of computer graphics, mesh-based techniques have been widely used to design freeform lenses for applications like controlling caustic patterns [1–3]. These methods model lens surfaces using triangle meshes (i.e., discrete 3D vertices connected by edges to form triangle faces). This allows for more precise representations of complex geometries than traditional methods, which typically involve solving partial differential equations over fixed grid points. Mesh-based designs have successfully produced lenses capable of generating complex caustic patterns resembling specific target images. However, existing approaches are limited to optimizing only one side of the lens, failing to fully utilize the degrees of freeform offered by freeform lenses. Moreover, they only aim at the caustic pattern on a single plane, which cannot fully control the outgoing light field. In this paper, we propose a novel approach that optimizes both sides of the lens. This enables controlling caustic patterns on more than one plane, providing new possibilities in light control applications.

2 Method

As an example problem, we consider a square-shaped double-sided lens, with a uniform parallel white light source in direction $\mathbf{d} = (0, 0, -1)$. The two sides of the lens are height fields over a domain $U = [0, h]^2$ in the xy-plane. The lens produces a caustic pattern on a receptive plane $\mathcal{P}$ orthogonal to $\mathbf{d}$. We optimize the lens shape so that the caustic pattern inside the area $I = \{(x, y, z) \in \mathcal{P} \mid (x, y) \in U\}$ resembles a target image. We assume that there exists a bijective map between the two sides of the lens, such that each light ray striking a point on the front surface will then strike its corresponding point on the back surface. Therefore, we represent the two sides using two triangle meshes $\mathcal{M}_1, \mathcal{M}_2$ with the same topology (i.e., they have the same number of vertices connected in the same way), where the elements of the two meshes are in one-to-one correspondence. From the bijectivity assumption, all incoming light rays striking a front surface triangle $\triangle \mathbf{v}_1^i \mathbf{v}_1^j \mathbf{v}_1^k \in \mathcal{M}_1$ are refracted to rays that strike a back surface triangle $\triangle \mathbf{v}_2^i \mathbf{v}_2^j \mathbf{v}_2^k$ with corresponding vertices. The rays are then refracted again at $\triangle \mathbf{v}_2^i \mathbf{v}_2^j \mathbf{v}_2^k$ to hit the plane $\mathcal{P}$ and form a caustic pattern. We approximate the pattern using a triangle $t_{ijk} = \triangle \mathbf{q}_i \mathbf{q}_j \mathbf{q}_k \in \mathcal{P}$ with uniform brightness, whose vertices are the intersection points between $\mathcal{P}$ and the refracted rays emitted from $\mathbf{v}_2^i$, $\mathbf{v}_2^j$ and $\mathbf{v}_2^k$ respectively. Assuming no energy loss during refraction, the total flux $\Psi(t_{ijk})$ of t_{ijk} is proportional to the projected area of the triangle $\triangle \mathbf{v}_1^i \mathbf{v}_1^j \mathbf{v}_1^k$ in the xy-plane. The caustic pattern for the whole lens is obtained by accumulating all such triangles $\{t_{ijk}\}$. To determine an intersection point $\mathbf{q}_i$, we note that the incoming ray for $\mathbf{v}_2^i$ is in the direction $\mathbf{a}_i = (\mathbf{v}_2^i - \mathbf{v}_1^i)/\|\mathbf{v}_2^i - \mathbf{v}_1^i\|$. We then introduce an auxiliary variable $\mathbf{n}_2^i \in \mathbb{R}^3$ for the surface normal direction at $\mathbf{v}_2^i$, and use Snell's law to compute the refracted ray direction at $\mathbf{v}_2^i$ as $\mathbf{b}_i = \overline{\mathbf{n}}_2^i \sqrt{1 + \eta^2((\overline{\mathbf{n}}_2^i \cdot \mathbf{a}_i)^2 - 1)} + \eta\,(\mathbf{a}_i - (\mathbf{a}_i \cdot \overline{\mathbf{n}}_2^i)\overline{\mathbf{n}}_2^i)$, where $\overline{\mathbf{n}}_2^i = \mathbf{n}_2^i/\|\mathbf{n}_2^i\|$, and η is the lens's reflective index.

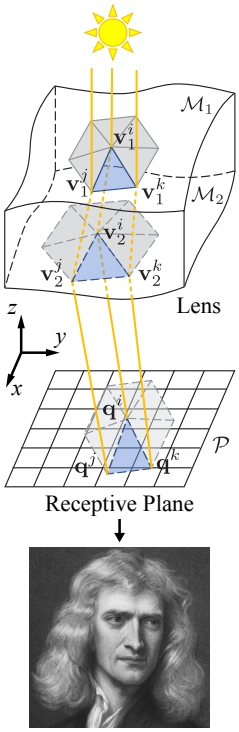

To compare the caustic pattern with the target image, we divide the imaging area I into a grid of square cells $\{p^l\}$ corresponding to the target image pixels. The flux contribution from a caustic triangle t_{ijk} to a cell p^l is

⋆ e-mail: yosun@mail.ustc.edu.cn
⋆⋆ e-mail: DengB3@cardiff.ac.uk
⋆⋆⋆ e-mail: juyong@ustc.edu.cn

$\Phi_l(t_{ijk}) = \Psi(t_{ijk}) \cdot A(t_{ijk} \cap p^l)/A(t_{ijk})$, where $A(\cdot)$ denotes the area. Summing the contributions from all caustic triangles, we obtain the pixel value at p^l as $g^l = \gamma^{-1}\left(\sum_{t_{ijk}} \Phi_l(t_{ijk})\right)$, where $\gamma^{-1}(\cdot)$ is the inverse gamma correction. We introduce an optimization target term to penalize the difference between the value g^l and image gradient $\mathbf{G}^l$ at each pixel p^l and their corresponding values $\widetilde{g}^l, \widetilde{\mathbf{G}}^l$ from the target image: $E_{\text{img}} = \sum_{p^l} (g^l - \widetilde{g}^l)^2 + \|\mathbf{G}^l - \widetilde{\mathbf{G}}^l\|^2$. Here, the closeness of the image gradient helps to retain the image features.

In addition, the normals at mesh vertices must be compatible with the vertex positions. Thus, we adapt a compatibility term from [4]: $E_{\text{comp}} = \sum_{e \in \mathcal{E}} \overline{\mathbf{e}} \cdot (\overline{\mathbf{n}}_1^e + \overline{\mathbf{n}}_2^e)/\|\overline{\mathbf{n}}_1^e + \overline{\mathbf{n}}_2^e\|$, where $\mathcal{E}$ denotes the set of mesh edges in $\mathcal{M}_1$ and $\mathcal{M}_2$, $\overline{\mathbf{n}}_1^e$ and $\overline{\mathbf{n}}_2^e$ are the unit normals at the two vertices of the edge e, and $\mathbf{e}$ is the unit vector of e. This term requires the averaged vertex normal of each edge to be orthogonal to the edge. The vertex normals for $\mathcal{M}_2$ are derived from the auxiliary variables, while the normal $\mathbf{n}_1^i$ at each vertex $\mathbf{v}_1^i$ of $\mathcal{M}_1$ is computed from its incoming and outgoing ray directions $\mathbf{d}$ and $\mathbf{a}_i$ as: $\mathbf{n}_1^i = (\mathbf{d} + \eta\, \mathbf{a}_i)/\|\mathbf{d} + \eta\, \mathbf{a}_i\|$.

We also enforce some hard constraints for physical feasibility: (1) to prevent flipped triangle faces, we require each triangle on $\mathcal{M}_1$ and $\mathcal{M}_2$ to have a positive signed area when projected onto the xy-plane; (2) for each vertex on $\mathcal{M}_2$, we require the angle between its normal and its incoming ray to be smaller than a threshold, to prevent total internal reflection. We introduce a term E_{barr} that sums a set of logarithmic barrier functions enforcing the constraints.

Our overall optimization problem is written as

$$\min \quad w_1 E_{\text{img}} + w_2 E_{\text{comp}} + w_3 E_{\text{barr}}, \tag{1}$$

where w_1, w_2, w_3 are weights. We numerically solve this problem with an L-BFGS solver. After the optimization, we use the method of [5] to reconstruct two dense meshes that smoothly interpolate the vertex positions and normals of $\mathcal{M}_1$ and $\mathcal{M}_2$ respectively, to obtain the final lens shape.

3 Results and Discussion

Fig. 1 shows two examples of lenses designed using our method with acrylic material (η=1.49). In each example, both $\mathcal{M}_1$ and $\mathcal{M}_2$ contain 472,785 vertices and 942,816 triangles. The side length h of the lens is set to 10cm, and its thickness is approximately 2cm. To verify the lens design, we simulate the caustic pattern using LuxCoreRender, an established physically based renderer. We also visualize the surface shape of $\mathcal{M}_1$ and $\mathcal{M}_2$ using a color map of the relative height function $H(x, y) = z(x, y) - z_{\min}$, where $z_{\min}$ is the minimum z-coordinate of the surface.

At the top of Fig. 1, we use a Newton portrait as the target image, and the receptive plane is 60cm away from the lens. Similar to existing methods [1–3], the rendered caustic pattern of our lens closely resembles the target. The bottom part of Fig. 1 further demonstrates our method's capability to control more than one caustic pattern, which cannot be achieved with existing mesh-based approaches. Here, we use two target images showing the numbers 5 and 6, at the distance of 60cm and 120cm respectively. For such multi-target optimization, the term E_{img} in Eq. (1) considers all target images. The rendered caustics of the resulting lens maintain a strong resemblance to both target images. This example confirms the effectiveness of our method in utilizing the full degrees of freedom from freeform lenses to achieve complex effects.

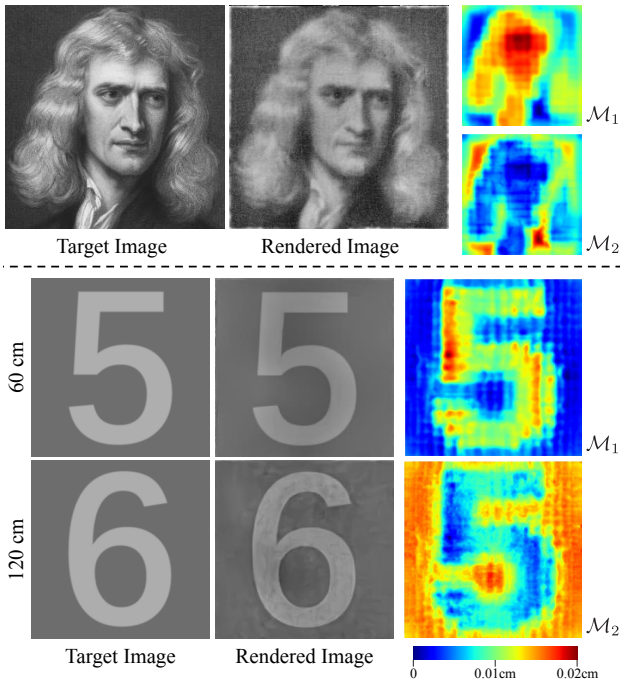

Figure 1. Examples of lens design created by our method. Top: a lens designed with one target image placed 60cm away from the lens. Bottom: a lens designed with two target images placed at 60cm and 120cm distance, respectively. The color maps show the relative height function for each side of the lens.

Our method can be improved and extended in the following aspects. First, to achieve even better optimization results, we will investigate its initialization strategy, such as the optimal transport approach from [1]. In addition, our method can be used to create lenses for general light control. In particular, we may specify a target light field using its caustics on multiple planes, and use these as targets to optimize the lens. Such capability can open up new possibilities for freeform optics design.

References

[1] Y. Schwartzburg, R. Testuz, A. Tagliasacchi, M. Pauly, ACM Trans. Graph. **33**, 74 (2014)
[2] Y. Yue, K. Iwasaki, B.Y. Chen, Y. Dobashi, T. Nishita, ACM Trans. Graph. **33**, 31 (2014)
[3] J. Meyron, Q. Mérigot, B. Thibert, ACM Trans. Graph. **37**, 224 (2018)
[4] X. Sun, C. Jiang, J. Wallner, H. Pottmann, in *Advances in Discrete Differential Geometry* (Springer, 2016), pp. 267–286
[5] M. Kazhdan, H. Hoppe, ACM Trans. Graph. **32**, 29 (2013)